The structural disorder of a silica network probed by site selective luminescence of the nonbridging oxygen hole centre

2010 J. Phys.: Condens. Matter 22 235801

(http://iopscience.iop.org/0953-8984/22/23/235801)

J. Phys.: Condens. Matter **22** (2010) 235801 (6pp) doi:10.1088/0953-8984/22/23/235801

The structural disorder of a silica network probed by site selective luminescence of the nonbridging oxygen hole centre

L Vaccaro and M Cannas

Dipartimento di Scienze Fisiche ed Astronomiche, Università di Palermo, Via Archirafi 36, I-90123 Palermo, Italy

E-mail: lavinia.vaccaro@fisica.unipa.it

Received 6 March 2010, in final form 7 April 2010
Published 21 May 2010
Online at stacks.iop.org/JPhysCM/22/235801

Abstract

We studied the inhomogeneous distribution of the luminescence band associated with the nonbridging oxygen hole centre in silica through site selective excitation/detection of the zero phonon line by a tunable laser source. Defects induced in the bulk of synthetic samples by γ and β exposure exhibit an increase of the inhomogeneous width from 0.071 to 0.086 eV on increasing the irradiation dose from 2×10^6 to 5×10^9 Gy. We also investigated two defect variants stabilized at the surface of the silica nanoparticles, $(\equiv Si–O)_3Si–O^\bullet$ and $(\equiv Si–O)_2(H–O)Si–O^\bullet$, whose inhomogeneous width was measured to be 0.042 eV and 0.060 eV, respectively. These results can be accounted for by the structural disorder around the defect, and specific causes of its variation can be pointed out, such as the network modification induced by irradiation or the structural alteration near the SiO_4 coordination sphere.

(Some figures in this article are in colour only in the electronic version)

1. Introduction

There has been long-standing interest in characterizing the optical transitions associated with the point defects in amorphous silica because of their practical relevance to several high-tech devices in the last few decades [1, 2]. As paradigmatic examples, defects cause a transmittance loss in optical fibres [3] or the emission of nano-sized particles exploited in optoelectronics or display technology [4]. In accordance with the spectroscopic viewpoint, both the optical absorption (OA) and the photoluminescence (PL) spectra result in overlapping broad bands, their widths being 0.1–1 eV, whose lineshape is influenced both by the homogeneous properties, related to a single defect, and by the inhomogeneous properties, due to the different interactions of each defect with the embedding matrix [5]. The inhomogeneity is therefore related to the structural disorder of the silica network in the long- and local-range in comparison with the SiO_4 tetrahedron size. The first is intrinsic to the amorphous state, and is mainly accounted for by the statistical distribution of the Si–O–Si bond angle and the size of $(Si–O)_n$ ring structure [6, 7]. The second is due to the presence of point defects that introduce a local distortion into the surroundings, such distortion being dependent on the site [8].

The attempt to single out homogeneous and inhomogeneous properties is an age-old tricky problem in the physics of amorphous materials and impedes the knowledge both of the microscopic properties of defects and of their environment. In particular, silica provides a model system suitable to address this issue: the oxygen-dangling bond, $\equiv Si–O^\bullet$ [9], commonly named a nonbridging oxygen hole centre (NBOHC), combines propitious features. This defect is, in fact, common to bulk and surface silica; in both systems it exhibits a composite OA spectrum with bands peaked in the visible and ultraviolet, all of them being able to excite PL around 1.9 eV [10–12]. On the other hand, it exhibits a very weak coupling between its nearly coincident visible electronic transitions, OA at 2.0 eV and PL at 1.9 eV, and the phonon mode associated with the silicon-dangling oxygen stretching [9, 13]. The main experimental outcome arising from this property is the detectability of the purely electronic transition or zero phonon line (ZPL) under site selective excitation of inhomogeneously distributed centres, thus allowing the inhomogeneous curve to be drawn directly. The detection of the ZPL is therefore

a probe of the silica structure near the NBOHC, as already tested both in bulk [14, 15] and at the surface of silica samples [16]. In contrast, this potential is precluded for other defects in silica, because of the stronger phonon coupling of their optical transitions. In those cases the deconvolution between homogeneous and inhomogeneous broadening can be done indirectly by analysing some specific optical features, as for example the lifetime of the oxygen defect centres (ODC(II)) [17].

In this work we report on an exhaustive study of the inhomogeneous properties of NBOHC embedded in the bulk and at the surface of silica taking advantage of the sensitivity and selectivity of our experimental apparatus being able to detect ZPL under tunable laser excitation. The comparison between these two systems allows us to succeed in more purposes. In bulk silica, where NBOHC are induced by γ- and β-rays, we study the dependence of the inhomogeneous broadening on irradiation dose in order to show the changes of the matrix under the action of high energy photons or particles. For surface silica two variants of NBOHCs were stabilized in films of nano-sized particles with high specific surface area. In the first, $(\equiv\text{Si–O})_3\text{Si–O}^\bullet$, each ligand O is bonded to two Si; in the second, $(\equiv\text{Si–O})_2\text{(H–O)Si–O}^\bullet$, one of the ligand O atoms is terminated by a H. In this case we make use of a twofold clue to address the inhomogeneity sources: (i) dangling oxygen at the surface does not experience any interaction with atoms in front of it, differently from the bulk; (ii) the comparison between the two surface-NBOHC variants allows us to evaluate the increase of inhomogeneity due to the alteration of the structure adjacent to the Si coordination sphere.

2. Methods

2.1. Theoretical background

To outline our experimental investigation, we briefly review the basics of the site selective luminescence technique [18, 19]. We consider the interaction between the exciting light with photon energy E_{ex} and an ensemble of N noninteracting defects contained in an amorphous medium. Each defect contributes to the absorption through a homogeneous lineshape, $A(E_{ex} - E_0 - S\hbar\omega)$, governed by the coupling between the electronic transition and phonons: E_0 is the energy of ZPL, $\hbar\omega$ is the phonon energy, and S (Huang–Rhys factor) is the number of phonons generated. Due to the site-to-site non-equivalence of defects embedded in the amorphous silica networks, it can be assumed that the ZPL has an inhomogeneous distribution $w(E_0)$; the total absorption lineshape, $A_{tot}(E_{ex})$, is, therefore, the convolution:

$$A_{tot}(E_{ex}) = N \int A(E_{ex} - E_0 - S\hbar\omega)w(E_0)\,dE_0. \quad (1)$$

The radiative decay from the excited state originates the photon emission (luminescence) with energy $E_{em} \leqslant E_{ex}$. Within the linear electron–phonon coupling approximation, the luminescence homogeneous lineshape L is the mirror image of A relative to the ZPL at E_0 ($E_{em} + E_{ex} = 2E_0$); thus leading to the expression $L(E_0 - E_{em} - S\hbar\omega)$, E_0 being distributed by $w(E_0)$. The luminescence intensity is proportional to absorbed photons with a factor $\eta \leqslant 1$ (quantum yield) and is given by:

$$L(E_{ex}, E_{em}) = \eta N \int A(E_{ex} - E_0 - S\hbar\omega)w(E_0)\,dE_0 \times \int L(E_0 - S\hbar\omega - E_{em})w(E_0)\,dE_0. \quad (2)$$

For a peculiar subclass of defects having a very low electron–phonon coupling ($S \approx 0$), such as the case of NBOHC in silica, ZPL lies within the homogeneous lineshapes and it is possible to site-selectively excite a specific defect subset within $w(E_0)$. In this case, the site selective luminescence intensity is defined as:

$$I_{S.S.}(E_{ex}, E_{em}) = \eta N \int A(E_{ex} - E_0) \cdot L(E_0 - E_{em})w(E_0)\,dE_0. \quad (3)$$

At low temperature, when the condition $kT \ll \hbar\omega$ is satisfied, only the lowest vibrational level of the electronic states is populated, so that $E_{ex} > E_0$ and $E_{em} < E_0$. This implies that $A(E_{ex} - E_0)$ and $L(E_0 - E_{em})$ vanish for negative arguments and the site selective luminescence is detected with the emission resonant to excitation, $E_{ex} = E_{em} = E_0$. Equation (3) reduces to the ZPL intensity:

$$I_{ZPL}(E_0) = \eta N A(0) \cdot L(0) \times w(E_0) \quad (4)$$

thus allowing the direct measurement of $w(E_0)$.

2.2. Experimental details

Our study on the NBOHC's ZPL was performed on the following samples:

(1) Samples of two types of synthetic high-purity silica where bulk-NBOHCs are induced by irradiation [20]. In the first material, Suprasil 1 (S1) supplied by Heraeus [21] with Si–OH concentration of 5×10^{19} cm^{-3}, NBOHCs are prevalently generated by an *extrinsic* process consisting in the radiolysis of OH:

$$\equiv\text{Si–OH} \longrightarrow \equiv\text{Si–O}^\bullet + \text{H}. \quad (5)$$

In the second material, ED-C supplied by Tosoh Quartz [22] with Si–OH content less than 6×10^{17} cm^{-3}, NBOHC generation is an *intrinsic* process due to the radiolysis of strained Si–O bonds:

$$\equiv\text{Si–O–Si}\equiv \longrightarrow \equiv\text{Si–O}^\bullet + {}^\bullet\text{Si}\equiv \quad (6)$$

with the consequent generation of another intrinsic defect ($^\bullet\text{Si}\equiv$), known as the E' centre in specialized literature [23].

The samples utilized in our experiments are slabs with an optically polished 5×5 mm^2 surface and 0.5 or 1.0 mm thickness. NBOHCs were induced by exposure to γ- and β-irradiation [20], carried out using a ^{60}Co source (1.2 MeV) and a Van de Graff electron accelerator (2.5 MeV), respectively. Hereafter the samples will be referred to as S1 or ED-C followed by the accumulated γ or β irradiation dose. NBOHC concentration in bulk samples could be estimated on the basis of the intensity of the OA at 2.0 eV and its oscillator strength $f = 1.91 \times 10^{-4}$ [15], through Smakula's equation [5]; the values are reported in table 1 with an uncertainty of ∼15%.

Table 1. Peak position $\bar{E}_0$ and inhomogeneous width FWHM determined by the ZPL distribution of bulk-NBOHC in S1 and ED-C samples exposed to different doses of γ- and β-rays, together with the concentration, and of surface-NBOHC in porous films. The associated errors derive from the fitting procedures. For the sake of comparison the published data of two neutron irradiated S1 samples are included.

Typology	Sample	$\bar{E}_0$ (eV)	FWHM (eV)
Bulk	S1/γ (2×10^6 Gy) (4.2×10^{17} cm^{-3})	1.912 ± 0.001	0.071 ± 0.002
	S1/β (1.2×10^8 Gy) (2.0×10^{18} cm^{-3})	1.908 ± 0.001	0.078 ± 0.002
	S1/β (5×10^9 Gy) (3.2×10^{18} cm^{-3})	1.909 ± 0.001	0.086 ± 0.002
	ED-C/β (1.2×10^7 Gy) (6.0×10^{17} cm^{-3})	1.914 ± 0.001	0.073 ± 0.002
	ED-C/β (1.2×10^8 Gy) (1.6×10^{18} cm^{-3})	1.912 ± 0.001	0.074 ± 0.002
	ED-C/β (1.2×10^9 Gy) (2.0×10^{18} cm^{-3})	1.908 ± 0.001	0.079 ± 0.002
	ED-C/β (4.0×10^9 Gy) (4.0×10^{18} cm^{-3})	1.909 ± 0.001	0.084 ± 0.002
	S1/n (1.6×10^{17} n cm^{-2}) [15]	1.91	0.074
	S1/n (10^{20} n cm^{-2}) [14]	1.93	0.086
Surface	Film1 ($\equiv$Si–O)$_3$Si–O$^\bullet$	1.997 ± 0.002	0.042 ± 0.002
	Film2 ($\equiv$Si–O)$_2$(H–O)Si–O$^\bullet$	1.984 ± 0.002	0.060 ± 0.002

(2) Microporous films of silica nanoparticles with two variants of surface-NBOHCs. They were obtained by pressing highly dispersed Aerosil-300, a hydrophilic fumed silica with an average particle size of 7 nm, a pore size of 3–6 nm and a specific surface of $\sim 10^6$ cm^2 g^{-1}. A multi-step thermo-chemical method was applied to stabilize ($\equiv$Si–O)$_3$Si–O$^\bullet$ and ($\equiv$Si–O)$_2$(H–O)Si–O$^\bullet$ at the hydroxylated silica surface of our samples, hereafter named Film1 and Film2, respectively. The main reactions are: (i) surface hydroxyl groups, $\equiv$Si–OH, are substituted by methoxy, $\equiv$Si–OCH$_3$, after treatment in methanol vapour at $T = 700$ K; (ii) pyrolysis reactions at $T \geqslant 1050$ K firstly cause the transformation, $\equiv$Si–OCH$_3 \rightarrow$ Si–H + O=CH$_2$, and (iii) the generation of surface E' centres by breaking $\equiv$Si–H; (iv) the treatment in N_2O atmosphere above 750 K leads to the oxygen chemisorptions thus producing the NBOHCs in Film1. NBOHCs in Film2 are generated after two further steps: (v) the treatment in H_2 atmosphere at $T = 300$ K leads to the recombination of the first NBOHC variant, the produced free H atom reacts with the defect ($\equiv$Si–O$_2$)Si=O thus producing an E' centre, $\equiv$(Si–O)$_2$(HO)–Si$^\bullet$, with a ligand O atom terminated by a H; (vi) the treatment in N_2O atmosphere, similarly to step (iv), generates the second variant of NBOHC. To avoid any reaction of the surface centres with molecular species, each sample is placed in a pure silica container with a residual He atmosphere of 3–4 mbar.

PL time resolved experiments were performed using the following set up. Pulsed excitation light, (pulse width $\sim$5 ns, repetition rate 10 Hz), was provided by a VIBRANT OPOTEK optical parametric oscillator laser system, pumped by the third harmonic (3.50 eV) of a Nd:YAG laser. The laser photon energy was varied within the ZPL distribution, the laser linewidth being $\sim$0.001 eV. The laser beam intensity was monitored by a pyroelectric detector and was kept sufficiently low (1 mJ/pulse) to avoid saturation of the PL intensity [14]. The emitted light was spectrally resolved by a monochromator equipped with a 1200 grooves mm^{-1} grating that ensured a spectral slit width of 0.05 nm. Detection used an intensified charge coupled device camera driven by a delay generator (PIMAX Princeton Instruments). The acquisition time window W_T and the delay T_D with respect to the arrival of the laser pulse were set to be $W_T = 40$ μs and $T_D = 1$ μs so that any scattered laser light was completely suppressed in the emission spectra. The temperature was kept at 10 K using an Oxford-OptistatCF continuous-flow helium cryostat, equipped with four optical windows and controlled by an Oxford-ITC503 instrument.

3. Results and discussion

3.1. Bulk

In figure 1(a) we report a set of time resolved PL spectra measured in the sample Suprasil 1/β(5×10^9 Gy) at $T = 10$ K, with excitation energy stepwise incremented from 1.789 to 2.015 eV. Each spectrum is detected in the vicinity of the excitation energy and shows the resonant ZPL, whose width ($\sim$1 meV) is almost coincident with the laser line, thus proving the site selective excitation of inhomogeneously distributed NBOHCs. The broad band that still remains at energies lower than ZPL is due to nonselective excitation via the phonon sidebands associated with soft modes, also coupled with the defect whose frequency is at most a few hundred cm^{-1} [24]. From the spectra of figure 1(a) we derive the dependence of the ZPL intensity on the excitation energy (*ZPL excitation spectrum*); it is reported in figure 1(b). According to equation (4), this spectrum is proportional to the inhomogeneous distribution of the purely electronic transition $w(E_0)$, arising from the different local environment surrounding the NBOHC in amorphous silica. $w(E_0)$ is best fitted by a Gaussian curve, $\exp[-(E - \bar{E}_0)^2/2\sigma^2]$, centred at $\bar{E}_0 = 1.909 \pm 0.001$ eV with a full width at half maximum FWHM $= 2\sqrt{2 \ln 2} \times \sigma$ of 0.086 ± 0.002 eV (full line in figure 1(b)).

The same procedure has been used to obtain $w(E_0)$ in the other S1 and ED-C samples exposed to different doses of γ- and β-rays. It is reported in figure 2 superimposed on the experimental distributions of the ZPL intensities. We note that the absolute values $I_{ZPL}(E_0)$ are proportional to the NBOHC concentration, in agreement with equation (4). As concerns the spectral shape, regardless of the material type and the irradiation history, the experimental points demonstrate that the purely electronic transition energy of bulk-NBOHCs is distributed following a Gaussian curve. On increasing the irradiation dose such curves exhibit a slight red-shift

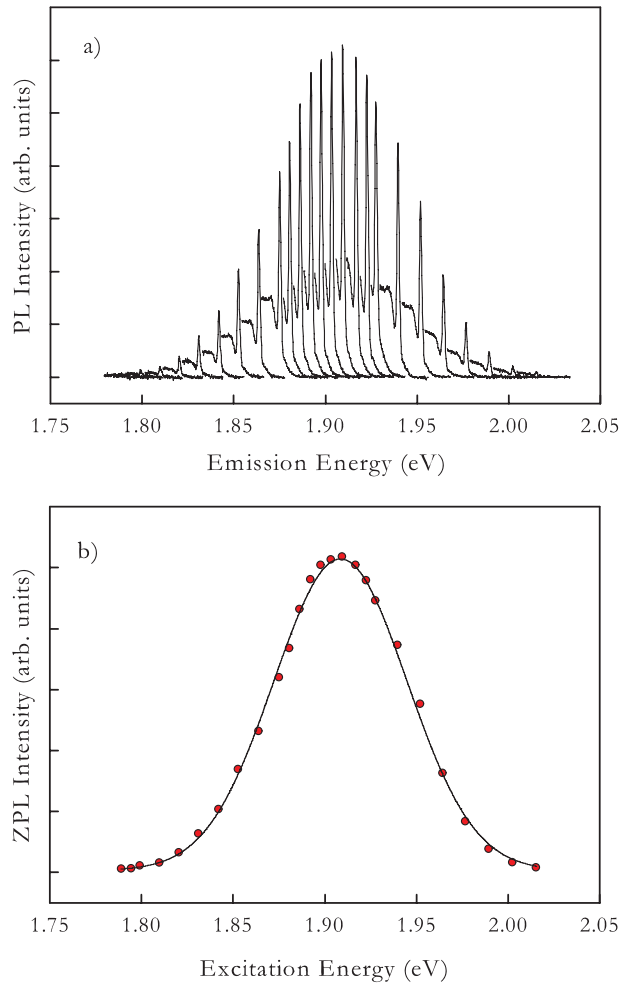

Figure 1. Panel (a): time resolved PL spectra measured in Suprasil $1/\beta(5 \times 10^9$ Gy) sample, at $T = 10$ K, at different excitation energies from 1.789 to 2.015 eV. Panel (b): distribution of the ZPL intensity obtained by the spectra reported in the panel (a) (red symbols) superimposed on a Gaussian best fit curve (solid line).

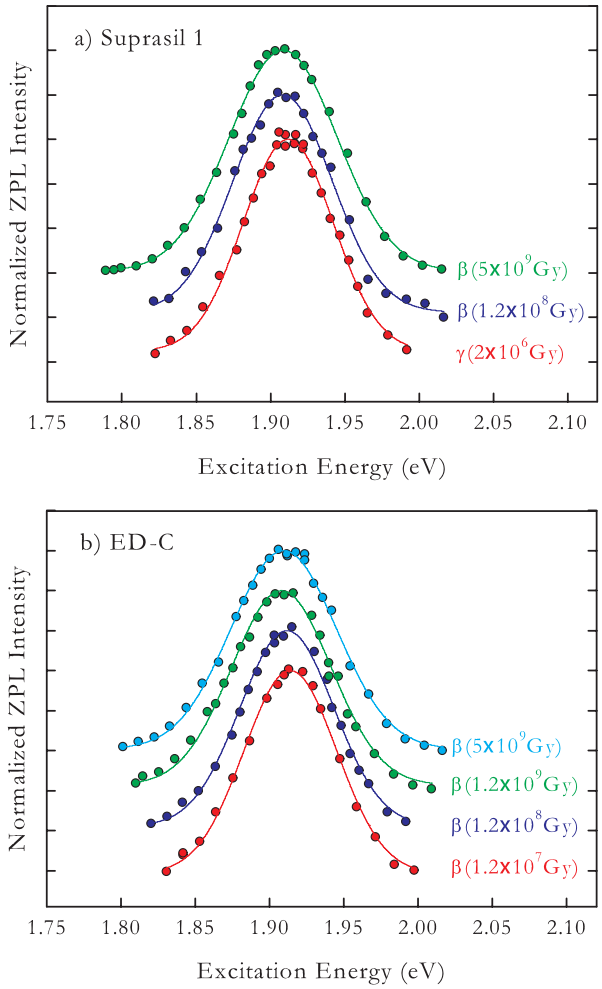

Figure 2. Distribution of the ZPL intensities measured in the Suprasil 1 and ED-C samples exposed to different doses of γ- and β-rays. Solid lines are the Gaussian best fit curves.

of their peak position and broaden: the values of $\bar{E}_0$ and FWHM obtained by the best fitting procedure applied to all the investigated samples are reported in table 1.

To better evidence the effect of irradiation on the broadening, in figure 3 the FWHM is also reported as a function of the γ- and β-doses. The inhomogeneous width increases with the irradiation dose; such trend, although limited to a few experimental points, is fairly similar for the two silica materials and therefore for both generation processes described by equations (5) and (6).

We acknowledge that previous site selective NBOHC luminescence experiments have addressed the inhomogeneous broadening measured by the ZPL distribution in synthetic wet silica differently irradiated with neutrons. Skuja in a sample exposed to 10^{20} neutrons cm^{-2} found a FWHM of 0.086 eV [14]; recently we have measured a FWHM of 0.074 eV in a sample irradiated with 10^{17} neutrons cm^{-2} [15], those results are also included in table 1. It is also worth noting that an increase of the inhomogeneous width was observed for the PL lineshape of ODC(II), induced by β irradiation [25]; in

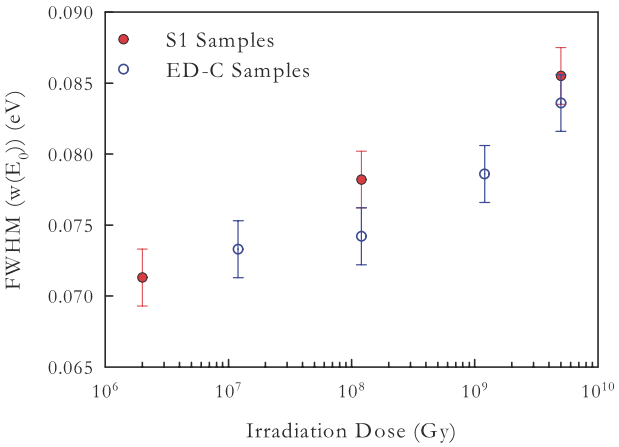

Figure 3. Inhomogeneous broadening as a function of γ and β irradiation doses detected in Suprasil 1 (full symbols) and ED-C (empty symbols) samples.

particular, after 5×10^9 Gy it increases by ≈60% in comparison with the native defects.

As a whole, these experimental findings indicate a quite common effect inherent in the generation of NBOHC

and ODC(II) in bulk silica: such defects experience an increasing inhomogeneity in increasingly irradiated samples. In particular, based on the peculiar capability of NBOHC to probe its environment, the width of the ZPL statistical distribution measures the disorder degree of the silica network, that is, how much the disordered matrix makes defects non-equivalent. We argue, therefore, that irradiation causes an increase of disorder around the NBOHC. It is worth noting that in [25], the analogous effect measured on ODC(II) was interpreted as due to: (i) progressive creation of new defects in sites with different geometrical configuration; (ii) progressive structural transformation of the silica host. Comparison with our results indicates, in the first case, that the statistical evolution of NBOHC configurations does not depend on the precursor site, OH or strained Si–O bond; a coincidence that weakens hypothesis (i). Help in settling this question comes from a recent work that, based on the change in the splitting of the primary ^{29}Si hyperfine doublet of the E' centres, shows an irradiation-induced densification around the defects [26]. We also remark that the observed red-shift of the ZPL distribution could be related to the induced irradiation transformation of the silica host around the defect that perturbs its electronic levels. Work is in progress to clarify the link between the densification and the effects on the inhomogeneous distribution.

3.2. Surface

In figure 4 we report the comparison between the inhomogeneous distributions $w(E_0)$ measured in Film1 and Film2 where $(\equiv$Si–O–$)_3$Si–O$^\bullet$ and $(\equiv$Si–O–$)_2$(HO–)Si(–O)$^\bullet$ are stabilized. The lineshape $w(E_0)$ is asymmetric for both films and is best fitted by a modified Gaussian curve, $\exp[-(E-\bar{E}_0)^2/2\sigma_H^2]$ for $E \geqslant \bar{E}_0$ and $\exp[-(E-\bar{E}_0)^2/2\sigma_L^2]$ for $E \leqslant \bar{E}_0$, the FWHM being $\sqrt{2\ln 2} \times (\sigma_L + \sigma_H)$. We get $\bar{E}_0 = 1.997 \pm 0.002$ eV with a FWHM of 0.042 ± 0.002 eV in Film1, and $\bar{E}_0 = 1.984 \pm 0.002$ eV with a FWHM of 0.060 ± 0.002 eV in Film2. In agreement with previous studies [27], the different peak position between the two surface-NBOHC variants reflects the influence of their symmetry on the electronic transition; this aspect is not central to the purposes of this work and will not be discussed in the following. In regard to the properties related to inhomogeneous broadening, the results of figure 4 point out: (i) regardless the surface-NBOHC variant, $w(E_0)$ is always narrower than that measured in the bulk defect; (ii) specifically, the substitution of a basal O with H increases the FWHM by ≈50%. The first point demonstrates that NBOHC at the surface experiences less disorder around it. A plausible justification arises from the nearly unperturbed nature of the dangling oxygen, which removes the sources of inhomogeneity in front of it. In fact, we recently demonstrated that the stretching frequency of the nearly free dangling oxygen at the surface is 920 cm^{-1} [16], against the value of 890 cm^{-1} measured in the same defect embedded in the bulk [14] where the electrostatic interaction reduces the force constant. To corroborate this hypothesis, we acknowledge studies on the vibrational features of SiOH groups in porous silica: noninteracting SiOH features a sharp peak at 3750 cm^{-1} whereas hydrogen-bonding interacting SiOH exhibits a broad composite band at lower energies [28, 29].

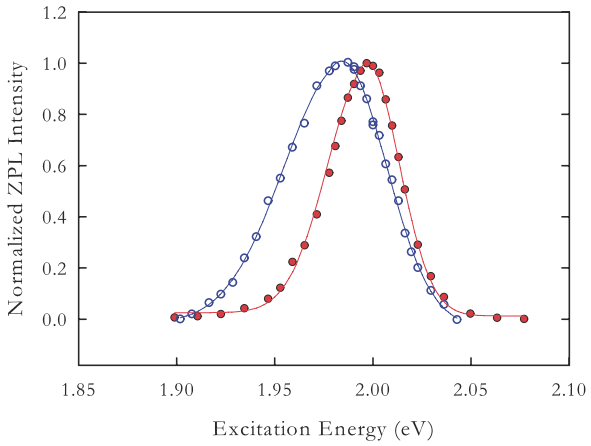

Figure 4. Distribution of the ZPL intensities measured in the Film1 (full symbols) and Film2 (empty symbols) samples. Solid lines are the modified Gaussian best fit curves.

The dominant cause of inhomogeneity for the surface-NBOHC is, therefore, the structural disorder of the matrix adjacent to the Si coordination sphere. Point (ii) is a direct proof of it, since it measures how much the alteration of the nearest-neighbour atom to the basal oxygen, caused by H, influences the inhomogeneous broadening of PL lineshapes. This evidence can also help to revaluate the disorder effects in the bulk, where the NBOHC structure is known only within the SiO_4 unit.

4. Conclusions

The investigation of the zero phonon line of NBOHC in silica has been successful in measuring how much the structural disorder experienced by the defect broadens the inhomogeneous distribution $w(E_0)$. In bulk samples, the dependence of the inhomogeneous width on the irradiation history indicates an increase of the disorder around NBOHC, likely due to progressive changes of the matrix. The comparison with the NBOHC stabilized in nanoparticles with high specific surface area provides a clue to singling out the inhomogeneity sources, both in front of the dangling oxygen and in the matrix adjacent to the silicon coordination sphere.

Acknowledgments

Financial support received from project ‘P O R Regione Sicilia—Misura 3.15—Sottoazione C’ is acknowledged. We would like to thank V Radzig (Semenov Institute of Chemical Physics of Moscow) for taking care of the preparation of the film samples and for enlightening discussions. We thank B Boizot for taking care of β irradiation at Ecole Polytechnique-Palaiseau (France). We are grateful to the members of the LAMP group (http://www.fisica.unipa.it//amorphous) for their support and stimulating discussions. Technical assistance by G Napoli and G Tricomi is also acknowledged.

References

[1] Pacchioni G, Skuja L and Griscom D L (ed) 2000 *Defects in SiO_2 and Related Dielectrics: Science and Technology* (Dordrecht: Kluwer Academic)

[2] Devine R A B, Duraud J P and Dooryhée E (ed) 2000 *Structure and Imperfections in Amorphous and Crystalline Silicon Dioxide* (New York: Wiley)

[3] Girard S, Meunier J P, Ouerdane Y, Boukenter A, Vincent B and Boudrioua A 2004 *Appl. Phys. Lett.* **84** 4215

[4] Uchino T and Yamada T 2004 *Appl. Phys. Lett.* **85** 1164

[5] Skuja L 2000 *Defects in SiO_2 and Related Dielectrics: Science and Technology* ed G Pacchioni, L Skuja and D L Griscom (Dordrecht: Kluwer Academic)

[6] Hobbs L W and Yuan X 2000 *Defects in SiO_2 and Related Dielectrics: Science and Technology* ed G Pacchioni, L Skuja and D L Griscom (Dordrecht: Kluwer Academic)

[7] Mauri F, Pasquarello A, Pfrommer B G, Yoon Y G and Louie S G 2000 *Phys. Rev.* B **62** R4786

[8] Hosono H, Ikuta Y, Kinoshita T, Kajihara K and Hirano M 2001 *Phys. Rev. Lett.* **87** 175501

[9] Skuja L 1994 *J. Non-Cryst. Solids* **179** 51

[10] Hosono H, Kajihara K, Suzuki T, Ikuta Y, Skuja L and Hirano M 2002 *Solid State Commun.* **122** 117

[11] Cannas M and Gelardi F M 2004 *Phys. Rev.* B **69** 153201

[12] Vaccaro L, Cannas M, Radzig V and Boscaino R 2008 *Phys. Rev.* B **78** 075421

[13] Suzuki T, Skuja L, Kajihara K, Hirano M, Kamiya T and Hosono H 2003 *Phys. Rev. Lett.* **90** 186404

[14] Skuja L, Suzuki T and Tanimura K 1995 *Phys. Rev.* B **52** 15208

[15] Vaccaro L, Cannas M and Boscaino R 2008 *Solid State Commun.* **146** 148

[16] Vaccaro L, Cannas M and Radzig V 2008 *Phys. Rev.* B **78** 233408

[17] D'Amico M, Messina F, Cannas M, Leone M and Boscaino R 2008 *Phys. Rev.* B **78** 014203

[18] Rebane K K 1970 *Impurity Spectra of Solids* (New York: Plenum)

[19] Funfschilling J, Zschokke-Granacher I and Williams D F 1981 *J. Chem. Phys.* **75** 3669

[20] Vaccaro L, Cannas M, Boizot B and Parlato A 2007 *J. Non-Cryst. Solids* **353** 856

[21] www.heraeus.com

[22] www.tosohquartz.com

[23] Skuja L 1998 *J. Non-Cryst. Solids* **239** 16

[24] Vaccaro L, Cannas M and Boscaino R 2008 *J. Lumin.* **128** 1132

[25] D'Amico M, Messina F, Cannas M, Leone M and Boscaino R 2009 *Phys. Rev.* B **79** 064203

[26] Buscarino G, Agnello S, Gelardi F M and Boscaino R 2009 *Phys. Rev.* B **80** 094202

[27] Vaccaro L, Cannas M and Radzig V 2009 *J. Non-Cryst. Solids* **355** 1020

[28] Anedda A, Carbonaro C M, Clemente F, Corpino R and Ricci C M 2003 *J. Phys. Chem.* B **107** 13661

[29] Yamada T, Nakajima M, Suemoto T and Uchino T 2007 *J. Phys. Chem.* C **111** 12973